

PROPORTIONAL COUNTER PHOTON CAMERA*

C. J. Borkowski and M. K. Kopp**
Oak Ridge National Laboratory
Oak Ridge, Tennessee 37830

MASTER

ABSTRACT

A gas-filled proportional counter camera that images photon emitting sources was built and tested. This camera measures and displays the impact location of individual photons in an energy range between 1 and 150 keV and permits pulse shape and energy discrimination for background reduction. Possible fields of applications for this camera include nuclear medicine, nuclear physics, x-ray diffraction, and related areas. The signal processing of the camera is based on further improvements and simplifications of the risetime method as applied to multiwire position-sensitive counters. Materials inside the counter were selected so that the camera can be used over long periods of time without purification of the counter gas.

The sensitive area of the camera is 200 x 200 mm², and the size of each picture element is 1 x 1 mm²; thus 40,000 picture elements are resolved. Counting rates of up to 20,000 photons/s do not appreciably affect the spatial resolution. The camera has been tested only with low energy photons (<30 keV) to determine the properties and applicability of the camera; however, by use of high pressure (>10 atm) Xe counter gas, a useful detection efficiency (>30%) and good spatial resolution are expected for 150-keV photons.

INTRODUCTION

A new type of photon camera was built and tested that images low energy photons (<150 keV) with a gas-filled, position-sensitive proportional multiwire counter as the photon detector. This camera has possible applications in the fields of nuclear medicine, nuclear physics, and x-ray diffraction.

The proportional counter photon camera has several advantages for imaging low energy photons: the pulse shape and energy of individual detected photons are measured to allow pulse shape and energy discrimination for background reduction; the electronic signal processing and image storage permit image enhancement and background subtraction; the dimensions of the sensitive area of the camera can be adapted to image large subjects, since the length of the multiwire electrodes and the number or spacing of the wires are practically unlimited; and the counter gas mixtures and pressures can be selected to detect a wide range of photon energies with adequate detection efficiency and good spatial resolution. Obviously, the camera can be adapted to detect and image other types of ionizing radiation, as, for example, electrons in chromatography experiments or neutrons in neutron diffraction experiments.

This work was limited to a camera of reduced size (200 x 200 mm² sensitive area) operating at low gas pressures (<150 cm Hg). It was tested only with low energy photons (<30 keV) to show the principle of operation and the characteristics of this type of camera.

*Research sponsored by the U. S. Atomic Energy Commission under contract with the Union Carbide Corporation.

**Denotes speaker.

The objectives of this work were to illustrate the adaptability and advantages of the risetime method^{1,2} in a photon camera, to investigate the improvements and simplifications in construction and signal processing that are possible with this method, and to construct and test a camera that has the required characteristics and, in addition, permits long-term operation without purification of the counter gas.

DESCRIPTION OF CAMERA

The camera has four main parts: collimator, gas-filled proportional counter, signal processing system, and display system (Fig. 1). The collimator, which is interposed between the subject to be imaged and the proportional counter, transmits only those photons that have a perpendicular trajectory with respect to the multiwire planes of the proportional counter and absorbs all other photons. The proportional counter detects a portion of the transmitted photons and produces electrical output signals proportional to the x-y coordinates and the energy of each detected photon. The signal processing and display systems transform the electrical signals and reproduce the image. A detailed description of the function, dimensions, and construction of the four parts of the camera follows.

Collimator

The channel collimator has a 120- x 160-mm² open area, an ~1-mm channel diameter, and a 25-mm height. The channel walls are 0.1-mm-thick copper. The collimator was assembled by stacking alternate flat and corrugated copper strips, 25 mm wide and 120 mm long, in a 25-mm-high frame with a 120- x 160-mm² opening.

The geometric efficiency of this collimator, i.e., the ratio of photons transmitted to photons emitted by the subject, is ~10⁻⁴. For a 100-mm spacing between the subject and the anode plane of the multiwire counter, the spatial resolution, i.e., the image diameter of one point of the subject, is 4 mm if all transmitted photons are detected at the anode plane. However, since part of the distance between the subject and the anode plane is in the counter gas, the effective distance between the points of photon emission and detection is reduced; and, therefore, the overall spatial resolution of the camera, when used with this collimator, is ~2 mm for a subject 100 mm above the anode plane. In this case, the collimator limits the resolution of the camera.

Proportional Counter

The position-sensitive proportional counter is housed in a 400-mm-diameter cylinder, which contains the counter gas, the multiwire anode and cathode frames, and a linear electron drift region (Figs. 2 and 3). The cylinder is closed at one end with a 20-mm-thick mounting plate that supports (1) the multiwire frames and the drift field electrodes on the inside of the counter, (2) the preamplifiers and high voltage filters on the outside, and (3) the feedthrough seals that connect the inside electrodes to the outside electronic circuits. The other end of the cylinder is closed with the photon entrance window.

The window is interchangeable and can be selected to permit the penetration of a wide range of photon energies and to contain a wide range of counter gas pressures. For most of the tests, which were performed with gas pressures < 2 atm, the window was 0.75-mm-thick aluminum.

The length of the cylinder can be varied to change the depth of the linear electron drift region, which therefore changes the detection efficiency of the camera for a given photon energy and counter gas composition or pressure. For all the tests, the cylinder was 100 mm long.

The linear electron drift region increases the detection efficiency, because it increases the amount of counter gas in the path of the transmitted photons and, therefore, the probability of interaction between photons and counter gas. The linear drift field causes the electrons produced by an interaction to drift toward the anode on a perpendicular path with respect to the anode wire plane, thus preserving the original coordinates of the interaction. The lateral boundaries of the linear drift field are defined by 200- x 200-mm² openings in a stack of parallel plates, or electrodes, spaced 12 mm.

The potentials of the electrodes are adjusted to create a constant voltage gradient perpendicular to the multiwire planes of the counter. The intensity of the potential field is adjusted for each counter gas mixture and pressure to obtain the maximum drift velocity of the electrons in the drift region.

The most negative electrode, which is closest to the entrance window, is covered with a 25- μ -thick aluminum membrane. This membrane transmits most photons and defines the upper boundary of the drift field, therefore limiting the active counting volume of the proportional counter. The least distance between the window and upper drift field electrode is 6 mm. The drift field plates are mounted on the multiwire frame assembly.

Three frames support the anode and cathode multiwire grids, with the anode plane centered between the two cathode planes. The space between the anode and cathode planes is 3 mm. The sensitive area of the grids is 200 x 200 mm². The upper cathode wires are orthogonal to the anode and lower cathode wires. The space between adjacent wires on all multiwire grids is 2 mm.

The construction of the multiwire grids was simplified considerably by the following method. Each grid was made with a single, continuous wire strung around a set of reference pins so that an interconnected set of 100 parallel, coplanar wires was formed. The cathode wires (75- μ -diameter Nichrome) were cemented to pretensioned springs with low outgassing epoxy without making any electrical connection between the wires and springs (Fig. 4). Similarly, the anode wires (12- μ -diameter stainless steel) were soft soldered to the pretensioned springs. The pretensioning rig and reference pins (not shown) were removed, and the wires remained supported under tension by the flat springs.

The main advantages of this construction method are: (1) the assembly time is short; (2) the wire spacing and coplanar assembly can be determined accurately by the reference pins; (3) only small amounts of outgassing insulating materials are present, since there are no electrical connections between individual wires and circuits outside the frames; and (4) the sets of 100 interconnected flat springs are fabricated in one operation by photo-etching 99 parallel strips, each 15 mm long and 0.2 mm wide, into 25-mm wide, 0.25-mm thick, and 200-mm long strips of

phosphor bronze.

Only one electrical connection to the anode grid and two electrical connections to each cathode grid are required when this method of construction and risetime signal processing are used. The counter gas mixture and pressure are selected to obtain adequate detection efficiency for the photon energy of the source to be imaged. We have used Ar, Kr, or Xe mixed with CH₄ at total pressures ≤ 2 atm.

Signal Processing Circuits

In the multiwire proportional counter and signal processing circuits (Fig. 5), the total resistance of each cathode between outputs is 6 k Ω , and the total capacitance between each cathode and the anode is 100 pF. For the signal flow, the cathodes can be considered as two orthogonal, lumped-element RC lines with 60 Ω resistance and 1 pF capacitance per wire segment with respect to the anode which is practically of signal ground for the frequency band of interest. The RC-line termination impedances Z_1 are rational fraction approximations to the characteristic impedance of the cathode RC lines.³ Methods for measuring the characteristic impedance of the cathodes and calculating the termination networks are given in the Appendix.

The functions and characteristics of the rest of the signal processing circuit are described in a previous paper.² The voltage sensitive preamplifiers⁴ are included in Fig. 5 in the functional block labeled "Filter and Crossover Detector."

In the following discussion the position-signal flow is described for a single photon detected at a point with coordinates x and y . In the detection process a localized electron avalanche is produced in the vicinity of the anode wire closest to y . The positive ions produced in the avalanche move toward the cathode planes and induce a displacement current in each cathode. These displacement currents are independent of the coordinates of the avalanche location; the sum of their magnitudes is proportional to the total charge Q_{in} of the avalanche and, therefore, proportional to the total energy loss of the detected photon. In addition, each type of ionizing event in the counter gas produces characteristically shaped displacement currents. This information can be used to reject unwanted background counts by energy and pulse-shape discrimination.

In each cathode the displacement currents divide into two equal parts and flow through portions of the cathode RC lines and through the termination networks to ground. The shapes of the currents in the termination networks and, therefore, the shapes of the voltages V_{x1} , V_{x2} , V_{y1} , and V_{y2} are functions of the length of RC line between the point of induction and cathode output. Therefore, if L is the total length of the cathode RC lines, the shapes of V_{x1} and V_{x2} are proportional to x and $L - x$, respectively; and the shapes of V_{y1} and V_{y2} are proportional to y and $L - y$, respectively. The shapes of these voltages are measured by crossover timing as described in a previous paper.²

The amplitudes of the time analyzer output signals in response to a detected photon are practically linear functions of the coordinates x and y . The position-sensitivity S , defined as the change in time analyzer output (ΔN) per unit length (ΔL) of the counter, was determined empirically as

$$S = \Delta N / \Delta L = 2 K (R_0 C / \omega_0)^{\frac{1}{2}} \quad (1)$$

where K is the gain of the time analyzer, R_0 and C_0 are the resistance and capacitance per unit length of the cathode RC lines, and ω_0 is the center frequency of the filter network.

The energy loss of a detected photon in the counter gas, proportional to the total current in the anode, can be measured in two ways: (1) by adding the four voltages V_{x1} , V_{x2} , V_{y1} , and V_{y2} at the output of the preamplifiers or (2) by measuring directly the current that flows from the anode to ground with a low input impedance current- or charge-sensitive preamplifier.

Signal Display Systems

Images taken with the photon camera were stored and displayed by several data display and storage devices other than a two-parameter analyzer.²

The simplest system is an oscilloscope with a photographic camera that takes time exposed pictures of the oscilloscope traces. The horizontal and vertical deflection electrodes are connected, respectively, to x and y outputs of the time analyzers. A short unblanking pulse ($\sim 1 \mu\text{s}$) is applied to the control grid of the cathode ray tube after the deflection transients. Thus, oscilloscope traces with coordinates proportional to x and y are displayed on the oscilloscope and integrated on the camera film. Most of the images shown in this paper under "Experimental Results" were obtained this way. The advantages of such a system are low cost, good gray-scale capability, and continuous resolution. However, image monitoring and image processing for background subtraction or noise rejection are not practical.

A bistable storage scope was evaluated as an image monitor, connected and blanked in the same way as a standard oscilloscope. The advantage of this type of monitor is that it combines continuous resolution with real-time observation of the image. The lack of gray-scale and image-processing capabilities and the long deflection transient ($\sim 90 \mu\text{s}$ for 200-mm, full-scale deflection) are disadvantages.

Another device, a lithicon storage tube with TV monitor display, offers the greatest number of advantages: good gray-scale capability; short deflection transient ($10 \mu\text{s}$ full scale); 1200-TV-line resolution; contrast, intensity, and magnification control of the stored image; and choice of image display on the TV monitor or single-frame transfer to video tape for dynamic imaging, e.g., function studies of organs.

The input connections and unblanking of this lithicon system are identical to those of the first two devices; all three have been used simultaneously.

EXPERIMENTAL RESULTS

The camera was tested in a series of imaging experiments to measure linearity and spatial resolution, to illustrate contrast and uniformity, and to suggest some areas of application for the camera. Over a 4-month test with the same counter gas, no change in spatial resolution occurred.

The linearity of the photon camera is illustrated in Fig. 6, which shows two images of a perforated plate having 4-mm-diameter holes spaced 12 mm apart. In the right-hand image, the plate was rotated 90° with respect to the left-hand image to illustrate horizontal and vertical linearity and distortion-free reproduction. The perforated plate covered the entire sensitive

area of the camera. The images were obtained with the channel collimator removed and the perforated plate placed directly on the window of the proportional counter. A point source of 22-keV x rays from ^{109}Cd was centered 150 cm above the window. The image was recorded on Polaroid film, with the time exposure display method described in the preceding section. The integral nonlinearity in both directions, x and y , is less than 1% of the sensitive area. (The dark spots in the upper left corner of Figs. 6, 9, and 10 are caused by the partial absorption of x rays in a gold film evaporated purposely on a small area of the inside face of the window.)

The spatial resolution of the camera without a collimator was measured with a perforated absorber plate (Fig. 7a). The plate was directly on the window, and the source configuration was the same as in the linearity test. The perforations in the plate were one row of 4-mm-diameter holes, four rows of 2-mm-diameter holes, and four rows of 1-mm-diameter holes. The spacings between holes in each row were twice the hole diameters. The rows of smaller diameter holes (1 and 2 mm) were grouped in orthogonal sets of two parallel rows each. The displacement of these rows along their main axes was 1 mm with respect to the corresponding parallel rows.

Figures 7b and 7c show the image of the absorber plate reproduced with the photon camera. Figure 7b was obtained by the time exposure method used for the linearity tests, and Fig. 7c is a photograph of the screen of the TV monitor connected to the lithicon storage system. The difference in these two reproductions shows clearly the image enhancement capability of the lithicon system.

The resolution test shows that the spatial uncertainty of the camera (without collimator) is approximately 1 mm in all directions, which is less than the anode wire spacing. Since the 1-mm displacement of the parallel rows of perforations is reproduced in the image of the absorber plate, and since the images of Figs. 8 through 11 do not show the characteristic structure of images from multi-wire detectors along the anode direction, we assume that the resolution of this camera is essentially continuous. This suggests that due to the finite track length of the 22-keV photoelectrons and the subsequent diffusion of the electrons in the drift region, electron clouds are produced which extend over several anode wires, resulting in simultaneous signals on these wires. Since the camera measures the position of the centroid of the charge distribution,¹ displacements smaller than one wire spacing in the direction across the anode wires can be detected.

The fidelity of reproduction of the hole pattern in the image of the absorber plate can be observed by comparing the small irregularities of the 1-mm-diameter hole spacing in the absorber with corresponding irregularities in the images.

The possible application of this camera in nuclear medicine is illustrated by the image of a standard Picker thyroid phantom⁵ on the TV monitor (Fig. 1). The image was produced with the channel collimator placed on the window and a 125 mm distance between the phantom and the anode. The phantom was filled with a 200- μC solution of ^{125}I which emits 29-keV x rays. The intensity of the x-ray emission from the phantom was modulated by several plastic absorbers incorporated in the phantom to simulate "hot" and "cold" nodules. The left lobe and the 11-mm-diameter "hot" nodule in the right lobe of the phantom had about twice the intensity of the left lobe. The diameters of the "cold" nodules, which did not emit x rays, were 4, 8, and 11 mm. All nodules were resolved in the image, and the difference in intensity is clearly shown. Some contrast was lost by x-ray scattering

in the plastic of the phantom. A total of 2×10^5 detected photons was accumulated to produce this image (including background).

Figures 8, 9, 10, and 11 illustrate the applicability of the camera to x-ray imaging problems where a low radiation dose is essential and the high resolution of x-ray film is not required. Shown are x-ray images of electric switches, scissors, the author's hand, and an etched pattern in the copper layer of a printed circuit board. The images were made using the time exposure display method. Each subject was placed on the window of the counter without the collimator, and a point source of 22-keV x rays from ^{109}Cd was centered 150 cm above the window. The images show the uniformity of response of the camera and the linear relation between subject and image. The radiation dose absorbed in producing the image of Fig. 11 was less than 10^{-6} rad!

OPERATING CHARACTERISTICS

The following is a brief summary of some of the operating conditions and characteristics of the photon camera.

- Sensitive area: $200 \times 200 \text{ mm}^2$.
- Active counter gas volume: 3 liters.
- Depth of counter gas volume: 75 mm.
- Counter gas mixture: 10% CH_4 + 90% Ar, Kr, or Xe.
- Counter gas pressure: 75-150 cm Hg.
- Spatial resolution:
 - a) Proportional counter: 1 mm in any direction (40,000 picture elements, tested with 22-keV photons in Kr- CH_4 at 150 cm Hg pressure).
 - b) Collimator: ~ 2 mm for a 125-mm distance between subject and anode plane.
- Integral nonlinearity: $< 2\text{mm}$.
- Counter detection efficiency: 65% for 30-keV photons in Kr- CH_4 at 150 cm Hg pressure.
- Collimator geometric efficiency: $\sim 10^{-4}$.
- Energy resolution (for 22-keV photons): 11% (fwhm) for a collimated point source; 35% (fwhm) for a source irradiating the entire sensitive volume of the detector.
- Count rate capacity (without pile-up rejection circuits): 20,000 counts/s, limited generally by the display system.
- Background count rate: 20 counts/s in Xe- CH_4 at 150 cm Hg pressure without additional shielding.
- Position signal processing time: $< 5 \mu\text{s}$ /photon.
- Bias (for 30-keV photons):
 - Anode-cathode: 2.1 kV in Ar- CH_4 at 150 cm Hg pressure; 3.5 kV in Xe- CH_4 at 150 cm Hg pressure.
 - Drift field: 40-60 V/mm.
- Electron drift velocity: $\sim 40 \text{ mm}/\mu\text{s}$ in Kr- CH_4 at 150 cm Hg pressure.
- Position sensitivity: $2.7 \times 10^{-2} \text{ V}/\text{mm}$.
- Time analyzer gain: $5 \times 10^6 \text{ V}/\text{s}$.
- Filter center frequency: $2 \times 10^6 \text{ radians}/\text{s}$.
- Position noise: $< 0.5 \text{ mm}$ (rms).

ACKNOWLEDGMENT

The authors acknowledge the assistance of the following ORNL personnel: J. A. Williams, G. W. Allin, and C. E. Fowler for their assistance in the construction of the proportional counters; R. S. Pressley and coworkers for preparing the radioactive sources; J. L. Lovvorn and coworkers for assistance in

adapting the PEP-400 Video/Graphic Storage Terminal⁶ for signal storage and display in the photon camera; and R. E. Zedler, W. A. Winchell, C. H. Nowlin, and R. J. Fox for many stimulating discussions.

APPENDIX

RC Line Characterization and Termination Network Calculations

The cathode RC-line characteristics are measured by the following procedure: (1) a conductance-capacitance bridge is connected to one cathode terminal, and (2) the other terminal of the same cathode is first short- and then open-circuited to measure the short- and the open-circuit impedances of the cathode. The characteristic impedance Z_0 of the RC line is the geometric mean of the short- and open-circuit impedances measured with the bridge

$$|Z_0| = R_{oc} R_{sc} \{ [1 + (R_{oc} C_{oc} \omega_m)^2] [1 + (R_{sc} C_{sc} \omega_m)^2] \}^{-\frac{1}{2}}, \quad (2)$$

where R_{oc} is the measured open circuit resistance in Ω , C_{oc} is the measured open circuit capacitance in F, R_{sc} is the measured short circuit resistance in Ω , C_{sc} is the measured short circuit capacitance in F, and ω_m is the measurement frequency of the capacitance bridge in radians/s. With the assumption that the cathode is approximately the distributed RC line, its impedance is⁷

$$Z_0 = (R_0/sC_0)^{\frac{1}{2}}, \quad (3)$$

where R_0 is the resistance in Ω /unit length, C_0 is the capacitance in F/unit length, and $s = \sigma + j\omega$ is the Laplace transform variable.

The resistance R_0 can easily be measured, and C_0 can be calculated from Eqs. (2) and (3). The frequency characteristic of the RC-line impedance Z_0 has a slope of 3 dB/octave. The function of the termination network is to match this frequency-impedance characteristic over a range necessary to extract the position information and, thereby, linearize the relation between subject and image dimensions.

One possible termination network resulting from a rational fraction approximation of Z_0^5 and its frequency characteristic are shown in Fig. 12. The network impedance has been normalized to 1 Ω at the center frequency ω_0 of 1 radian/s. The slope of the curve is approximately 3 dB/octave, which nearly matches the frequency characteristic of a distributed RC line ($Z_0 = 1 \Omega$ when $\omega = 1$ radian/s) over five octaves. The component values of Z_L can easily be scaled to any new value of Z_L at a given new center frequency ω_0 by making

$$R_n = r_n k_i \quad (n = 1, 2), \quad (4)$$

$$C_n = c_n (k_i k_\omega)^{-1} \quad (n = 3, 4, 5), \quad (5)$$

where $R_1, R_2, C_3, C_4,$ and C_5 are the component values of the scaled network; $r_1, r_2, c_3, c_4,$ and c_5 are the component values of the normalized termination network (Fig. 12); k_i is the new impedance of the termination network at the new center frequency in Ω , and k_ω is the new center frequency in radians/s.

References

1. C. J. Borkowski and M. K. Kopp, Rev. Sci. Instr. 39 (10), 1515 (1968).

2. C. J. Borkowski and M. K. Kopp, IEEE Trans. Nucl. Sci. NS-17 (3), 340 (1970).

3. C. H. Nowlin, ORNL, private communication.

4. M. K. Kopp, Rev. Sci. Instr. 42 (5), 714 (1971).

5. Picker X-Ray Corporation, White Plains, N. Y.

6. Princeton Electronic Products, Inc., North Brunswick, N. J. 08902.

7. D. K. Cheng, Analysis of Linear Systems, Addison-Wesley Publishing Co., Inc., Reading, Massachusetts, 1959, p. 368.

NOTICE

This report was prepared as an account of work sponsored by the United States Government. Neither the United States nor the United States Atomic Energy Commission, nor any of their employees, nor any of their contractors, subcontractors, or their employees, makes any warranty, express or implied, or assumes any legal liability or responsibility for the accuracy, completeness or usefulness of any information, apparatus, product or process disclosed, or represents that its use would not infringe privately owned rights.

LIST OF FIGURES

Fig. 1. Basic components and signal-flow diagram of a proportional counter photon camera. Shown are a Picker thyroid phantom (subject) and its image taken with the photon camera using channel collimator and lithicon storage tube-TV monitor display method.

Fig. 2. Drift field electrode and multiwire frame assembly of the position-sensitive proportional counter.

Fig. 3. Sectional view of the position-sensitive proportional counter.

Fig. 4. Multiwire frame with continuous wire grid assembly.

Fig. 5. Simplified diagram of the multiwire proportional counter and signal processing circuits.

Fig. 6. Two images of a perforated plate taken with the photon camera to illustrate linearity and lack of distortion.

Fig. 7. Spatial resolution test taken with the photon camera: (a) the hole pattern in the absorber plate; and its image as reproduced with the photon camera using (b) the time exposure method, and (c) the lithicon storage tube-TV monitor display method.

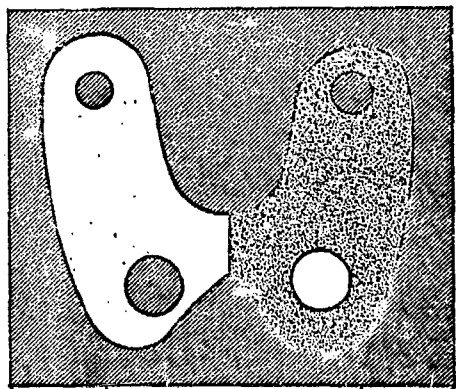
Fig. 8. X-ray image of a group of assorted electric switches taken with the photon camera with 22-keV ^{109}Cd x rays and time exposure display.

Fig. 9. X-ray image of scissors taken with the photon camera; the entire sensitive area is displayed to illustrate the uniformity in response of the camera. Radiation and display in Fig. 8.

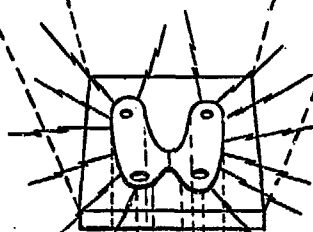
Fig. 10. X-ray image of the author's hand taken with the photon camera. Total radiation dose is $<10^{-6}$ rad. Radiation and display as in Fig. 8.

Fig. 11. X-ray image of an etched pattern in the copper layer of a printed circuit board taken with the photon camera. The image covers the entire sensitive area of the camera. Radiation and display as in Fig. 8.

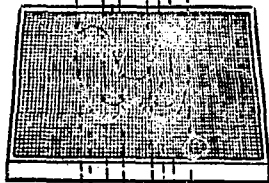
Fig. 12. Termination network with an impedance Z_L that is a rational fraction approximation of the characteristic impedance of an RC line (Z_0), and a graph of the impedances Z_L and Z_0 as functions of frequency.



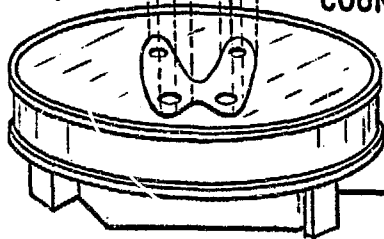
SUBJECT



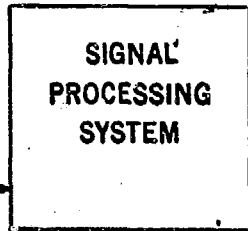
**THYROID
PHANTOM**



COLLIMATOR



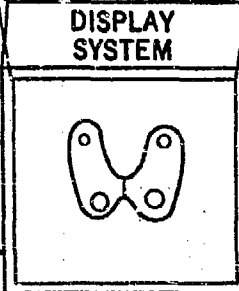
**PROPORTIONAL
COUNTER**



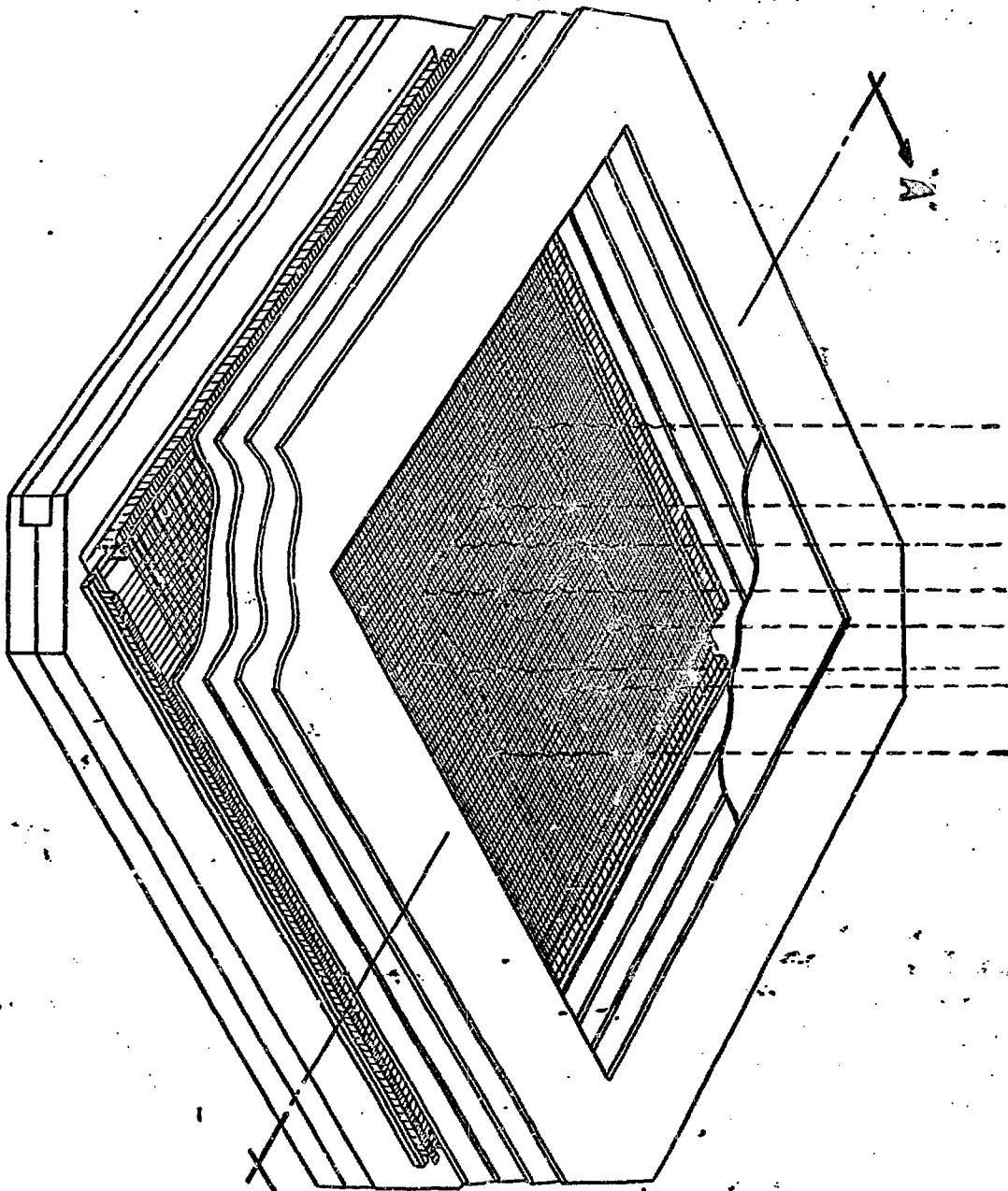
**SIGNAL
PROCESSING
SYSTEM**



IMAGE



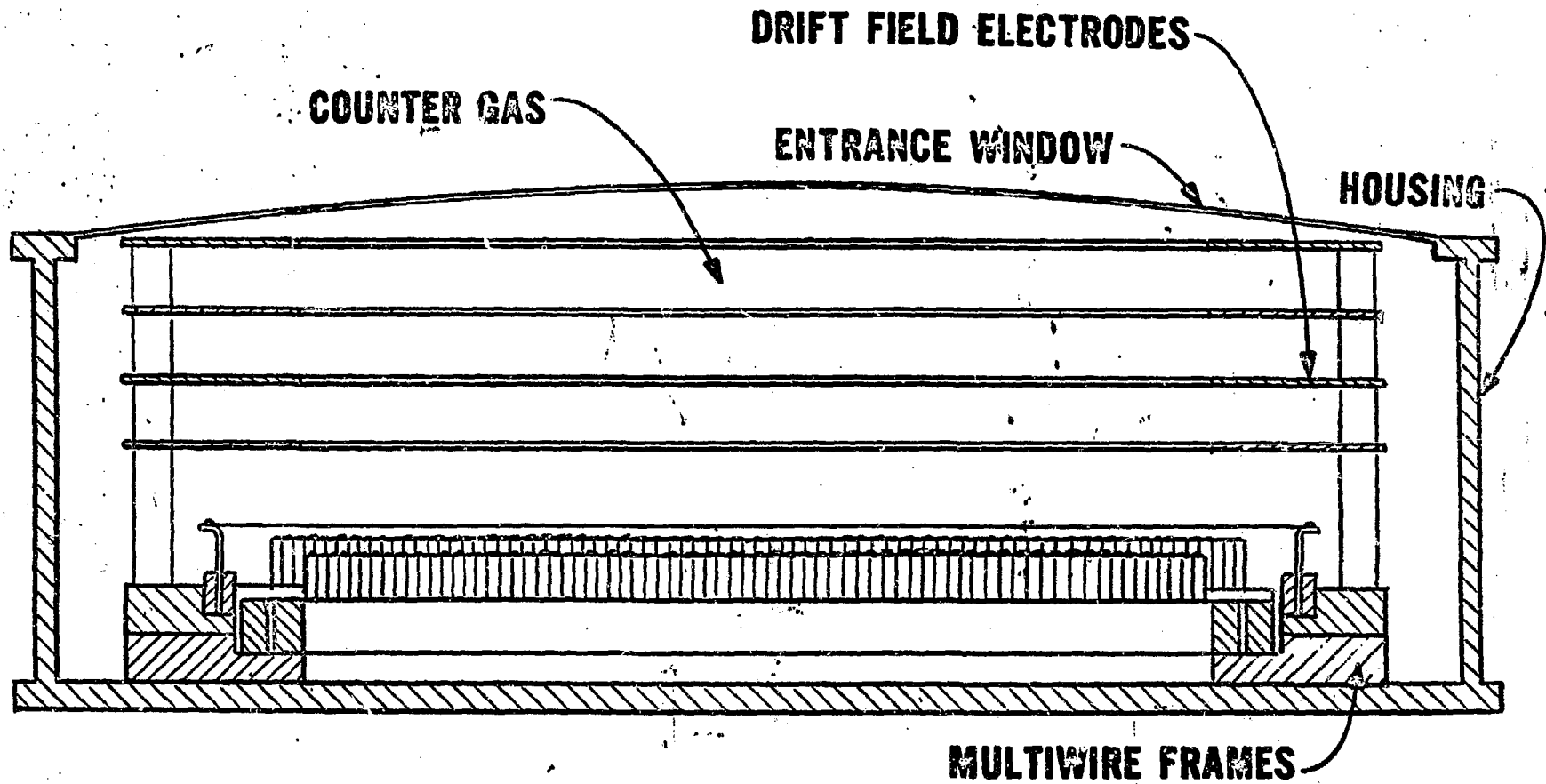
**DISPLAY
SYSTEM**



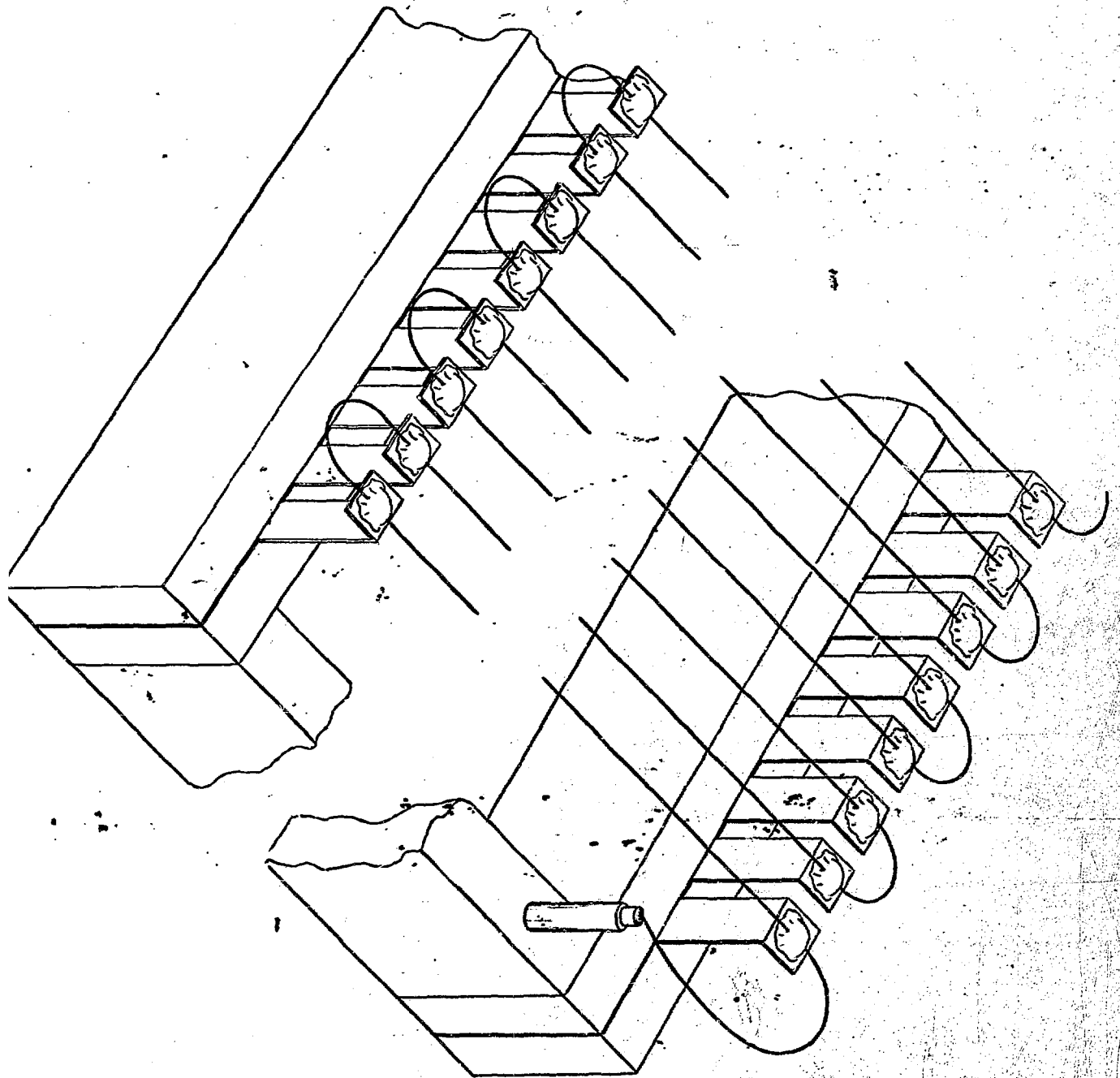
"A-A"

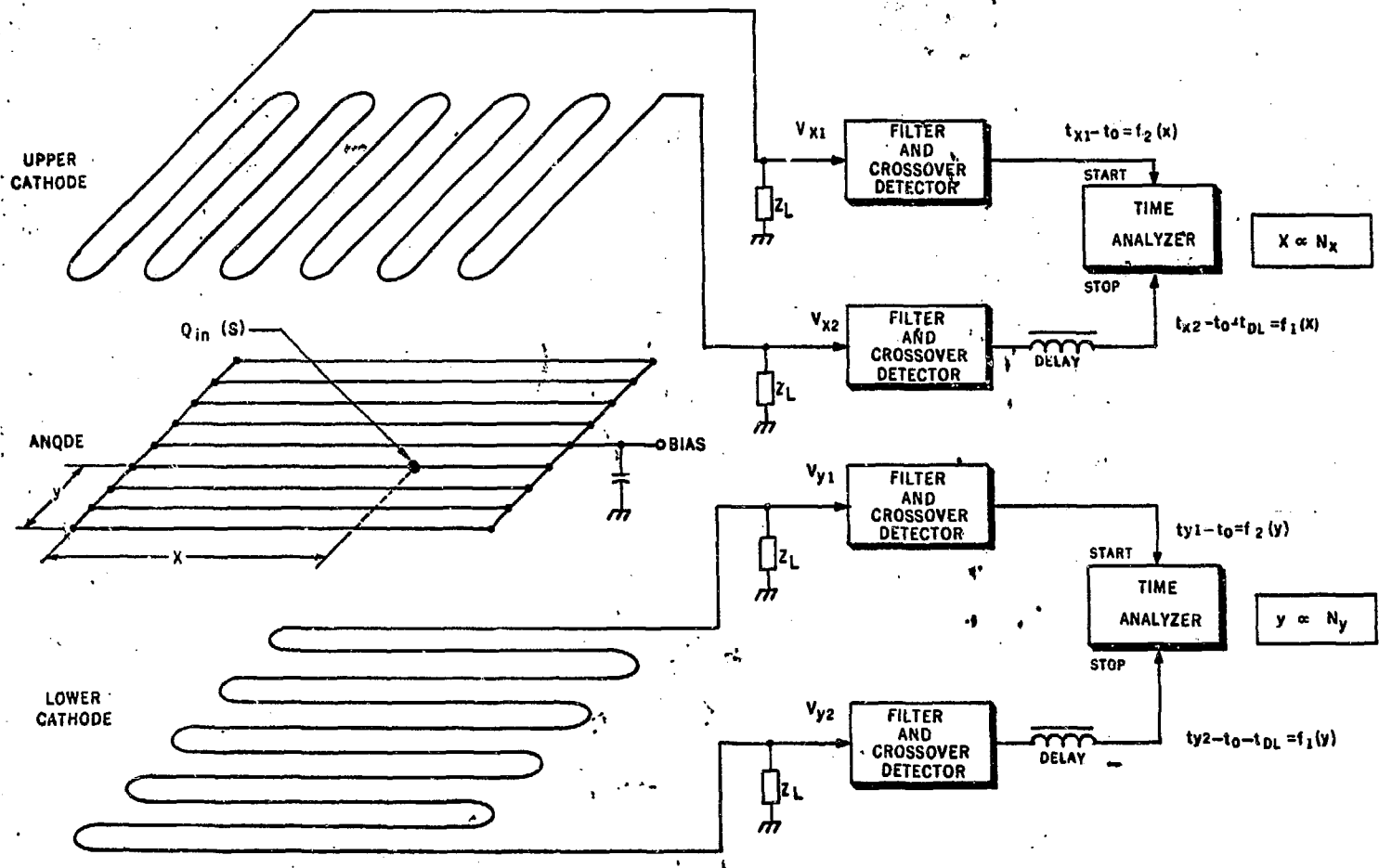
MULTIWIRES
FRAMES

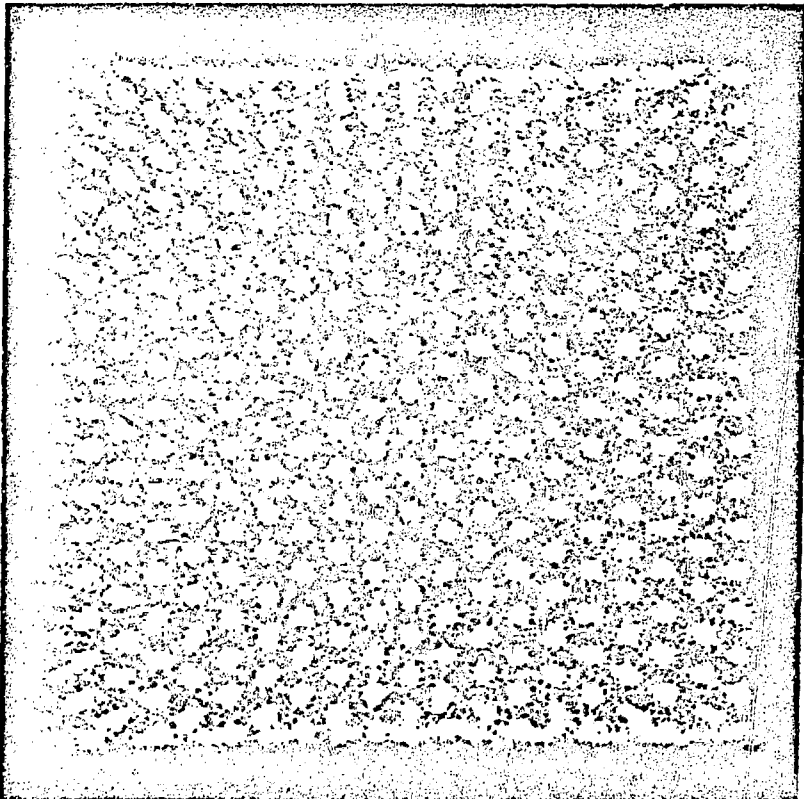
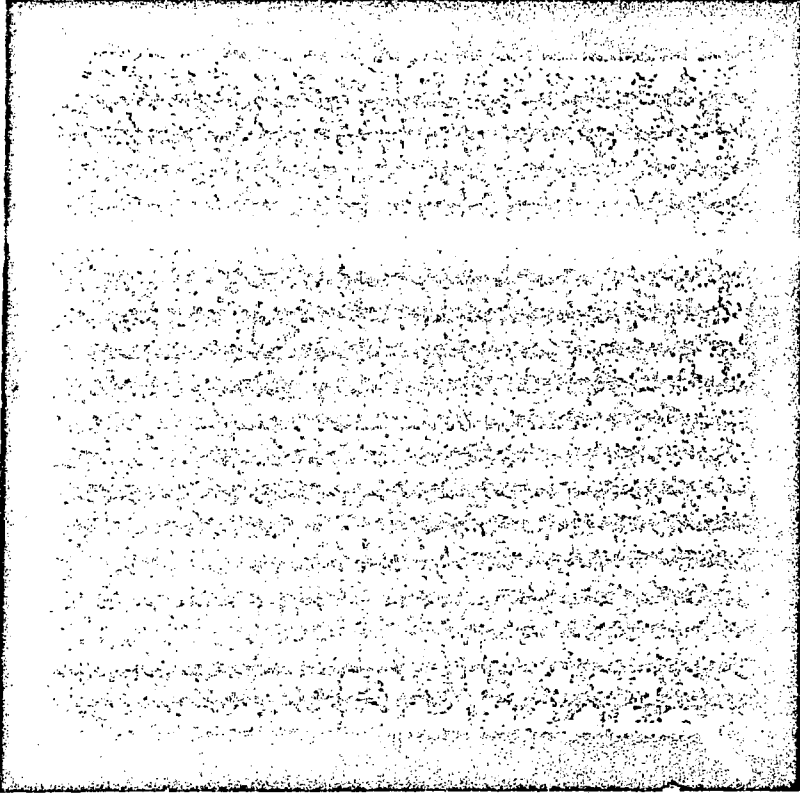
DRIFT FIELD
ELECTRODES

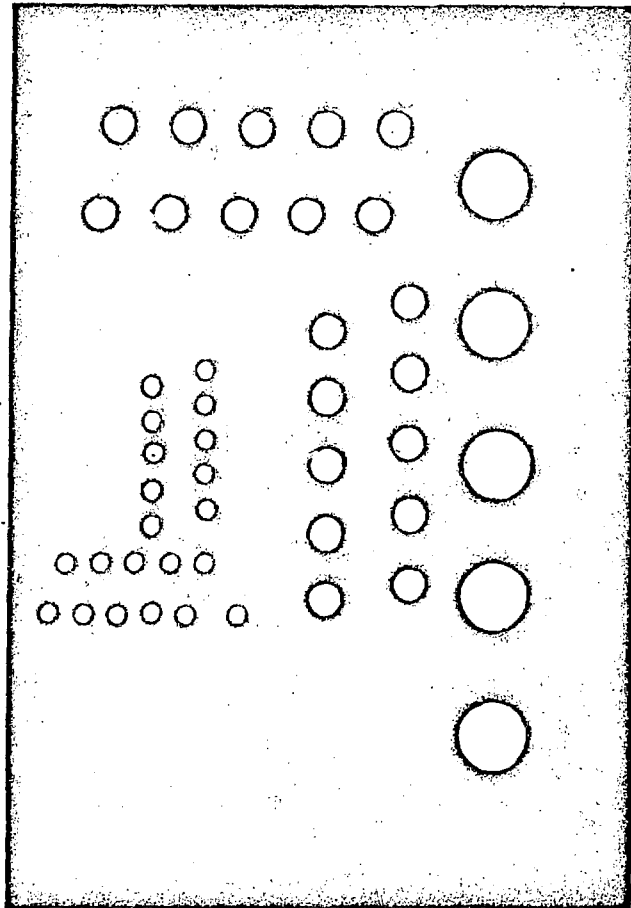


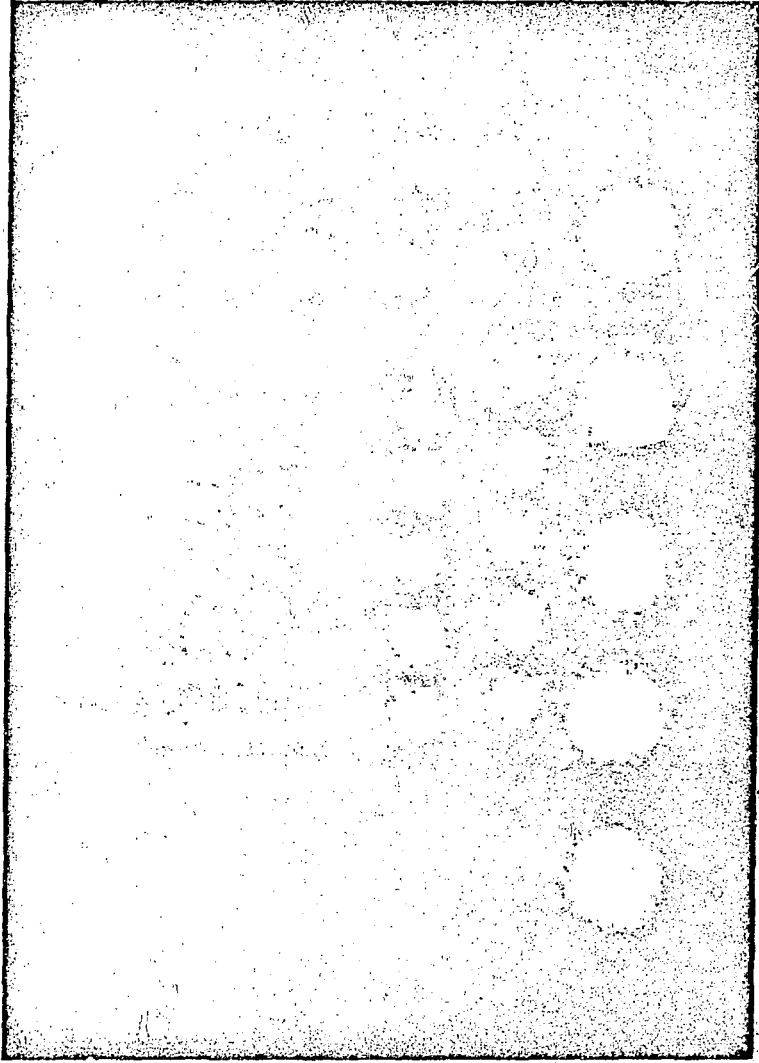
SECTION 'A-A'

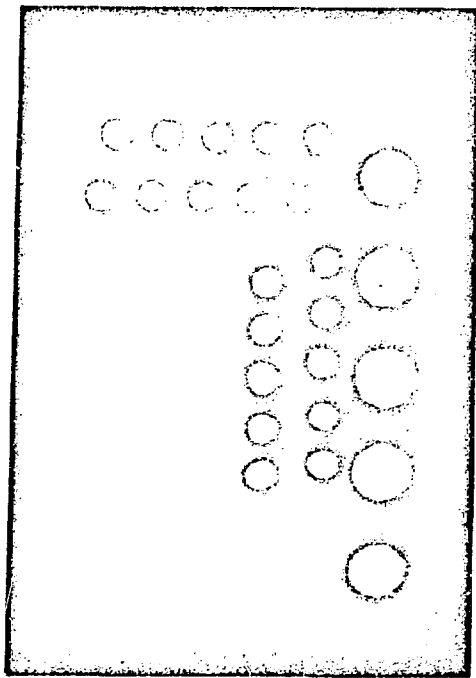


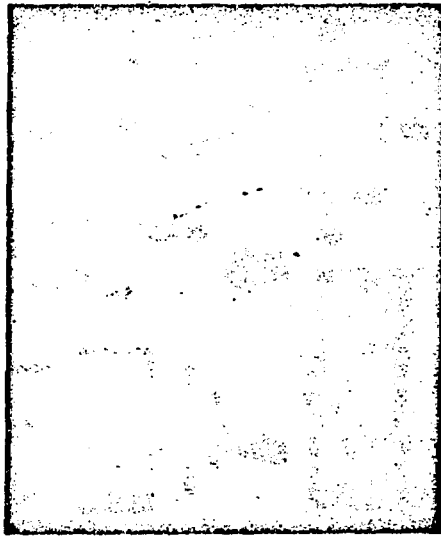


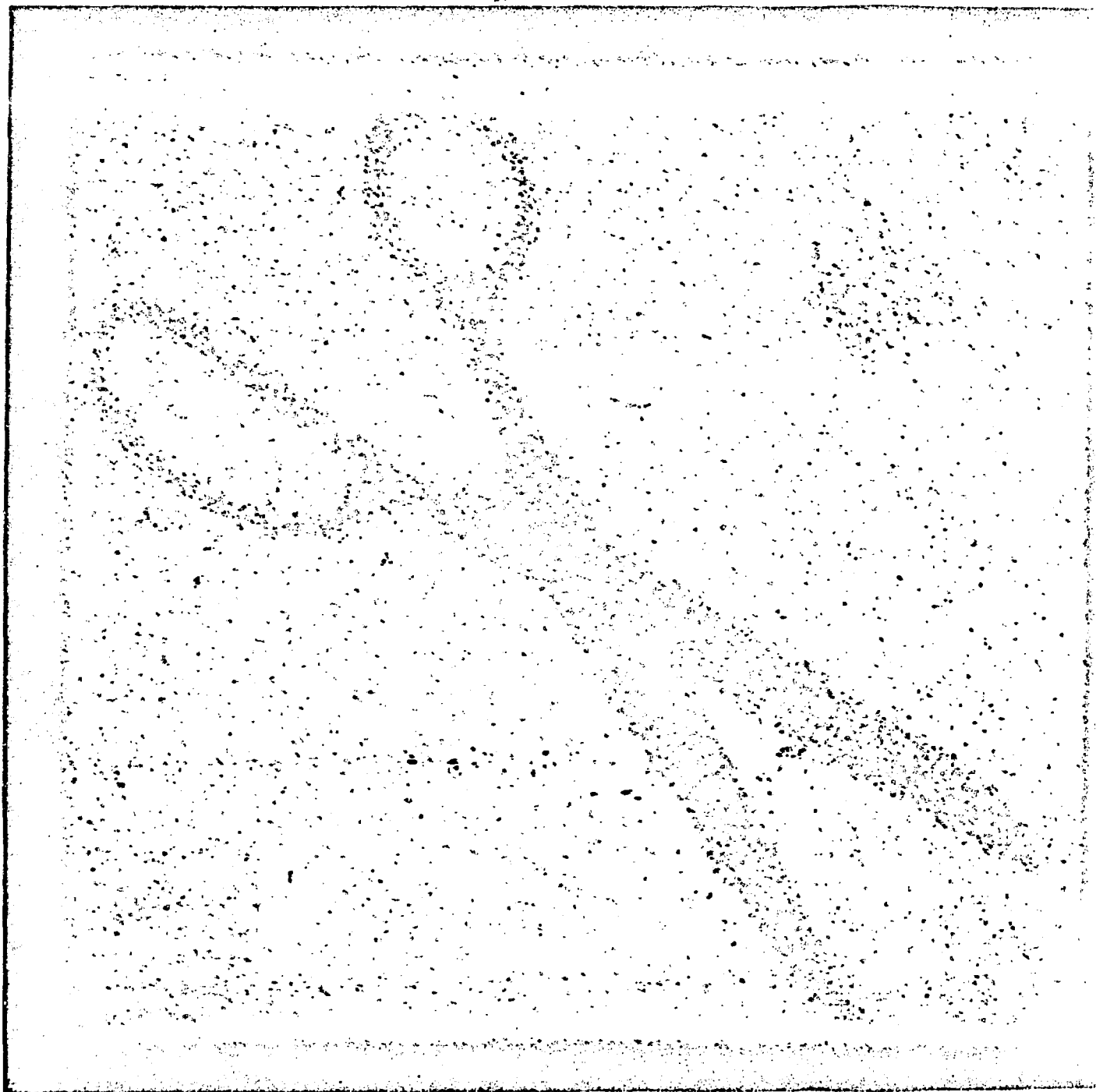


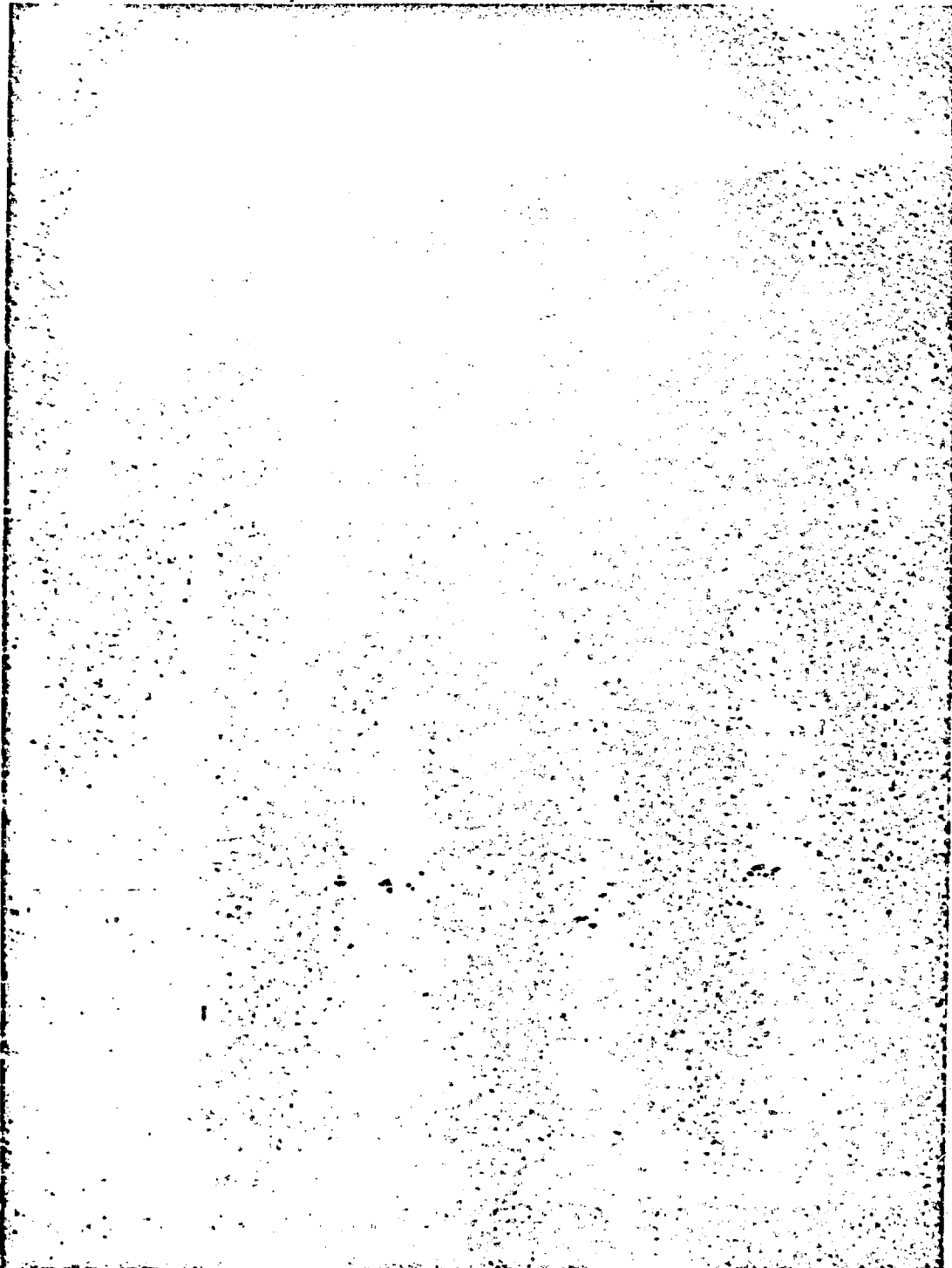


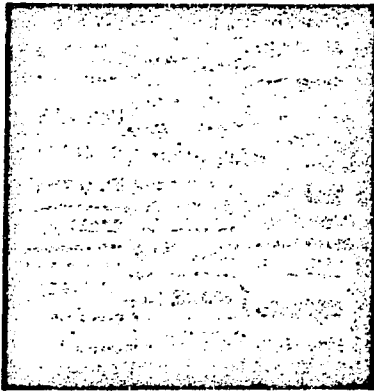












NORMALIZED IMPEDANCE (dB)

